High power density electrodes for Carbon supercapacitor applications

Cristelle Portet, Pierre-Louis Taberna, Patrice Simon, Emmanuel Flahaut, Christel Laberty-Robert

High power density electrodes for Carbon supercapacitor applications

C. Portet, P.L. Taberna, P. Simon, E. Flahaut and C. Laberty-Robert

CIRIMAT, UMR CNRS 5085, 118 Route de Narbonne; 31062 Toulouse Cedex, France

Abstract

This paper presents results obtained with 4 cm^2 Carbon/Carbon supercapacitors cells in organic electrolyte. In the first approach, a surface treatment for Al current collector foil via the sol–gel route has been used in order to decrease the Al/active material interface resistance. Performances obtained with this original process are: a low equivalent series resistance (ESR) of 0.5 Ω cm^2 and a specific capacitance of 95 F g^{-1} of activated carbon.

Then, supercapacitors assembled with treated Al foil and active material containing activated carbon/carbon nanotubes (CNTs) with different compositions have been studied. Galvanostatic cycling measurements show that when CNTs content increases, both ESR and specific capacitance are decreased. Fifteen percent appears to be a good compromise between stored energy and delivered power with an ESR of 0.4 Ω cm^2 and a specific capacitance of 93 F g^{-1} of carbonaceous active material.

Finally, cells frequency behaviour has been characterized by Electrochemical Impedance Spectroscopy. The relaxation time constant of cells decreases when the CNTs content increases. For 15% of CNTs, the time constant is about 30% lower as compared to a cell using pure activated carbon-based electrodes leading to a higher delivered power.

Keywords: Supercapacitors; Sol–gel route; Carbon nanotubes; Activated carbon; High power

1. Introduction

Energy storage devices are classified according to their energy and power densities. Supercapacitors are intermediate systems between dielectric capacitors and batteries. While batteries able to store higher energy density than supercapacitors, they deliver less power; as compared to dielectric capacitors, supercapacitors can store higher energy density with less delivered power. This particular properties make them suitable for numerous applications such as power electronics, spatial, military field; they can also be used in hybrid electric vehicle (HEV) in order to help the stop and go function, to provide peak power for improved acceleration, for energy recovery, … [1] and [2].

Three main classes of supercapacitors are described in the literature: metal oxide [3] and [4], electronically conducting polymer [5] and [6] and Carbon/Carbon supercapacitors [7] and [8]. Recently, hybrid supercapacitors have been developed where an activated carbon electrode is associated with a faradic electrode [9] and [10].

Carbon/Carbon supercapacitors have been largely investigated because of their low-cost, high cycling-life and high capacitance. Small (few farads) up to large-size (5000 F) devices are commercially available (Maxwell, Epcos, Panasonic, …) [11] and [12]. Highly-porous carbons are used as electrode material due to their high surface area, good electronic conductivity and high electrochemical stability; the most frequently used is activated carbon (1500–2000 $m^2\ g^{-1}$). Charge storage is performed through the reversible adsorption of the ions at the active material/electrolyte interface; no faradic reactions occur during the charge–discharge of the supercapacitor.

In this paper, the improvement of electrode material has been investigated for increasing power performances of Carbon/Carbon supercapacitors.

The first part of this paper presents performances of 4 cm^2 Carbon/Carbon supercapacitors assembled with treated Al current collectors; the aim of the treatment on the current collector is to improve the Al/active material interface properties in order to decrease the internal resistance. A two-step process is described; a chemical etching in order to increase the surface area of the foil is followed by a conducting film deposit via a sol–gel route.

In the second part of this paper, the influence of carbon nanotubes (CNTs) addition in the active material on supercapacitor performances has been studied. CNTs have particular properties which make them suitable for supercapacitor applications [13], [14] and [15]. Some authors reported performances of supercapacitors using CNTs-based electrodes in aqueous electrolyte. Specific capacitance remains lower than specific capacitance obtained with activated carbon (from 50 to 80 F g^{-1}) and several treatments have been proposed in order to increase the capacitance such as polymer deposit [16] and [17] or physical/chemical activation [17] and [18]. In this present work, CNTs used are double-walled carbon nanotubes (DWNTs); they are particular multi-walled carbon nanotubes (MWNTs) because they have a smaller number of concentric walls and they are attempted to have an intermediary behaviour between SWNTs and MWNTs. Performances of 4 cm^2 supercapacitors cells assembled with treated Al current collectors and active material containing activated carbon/CNTs mixture with different compositions are presented and discussed.

In the third part, the frequency behaviour of these cells was studied by Electrochemical Impedance Spectroscopy.

2. Experimental

2.1. Constitution of 4 cm^2 Carbon/Carbon supercapacitors cells

4 cm^2 supercapacitors cells are assembled by laminating active material on the Al current collector foil. The active layer composition is: 95 wt% activated carbon, 3 wt% CMC and 2 wt% PTFE (carboxymethylcellulose from Prolabo and polytetrafluoroethylene from Dupont de Nemours). The activated carbon used is the PicatifBP10 from the Pica Company (Vierzon, France). The active material weight is 60 mg. The process has been described elsewhere [19].

All the cell assembly is made in a glove box with both water and oxygen content lower than 1 ppm. The stack was assembled by inserting two layers of porous polymeric separators between the two electrodes. Two PTFE plates and stainless steel clamps are used in order to maintain the stack under pressure. The stack is immersed in an organic electrolyte, a solution of acetonitrile (AN, 10 ppm water) with 1.5 M NEt_4BF_4 dried salt.

2.2. Surface treatment of Al current collector

In a previous paper, we described the surface treatment of Al foil [19]. The etching process was based on previous work that has been developed for electrodes used in electrolytic capacitors in order to increase the surface area [20]. Firstly, an immersion of a 4 cm^2 Al foil in a NaOH solution was made to degrease the foil and to generate nucleation sites for Al dissolution. The foil is rinsed in distilled water and the etching treatment is performed in a HCl solution at 80 °C; the FEG-SEM picture (Fig. 1) shows the formation of channels in relation with a high controlled corrosion of the Al grains.

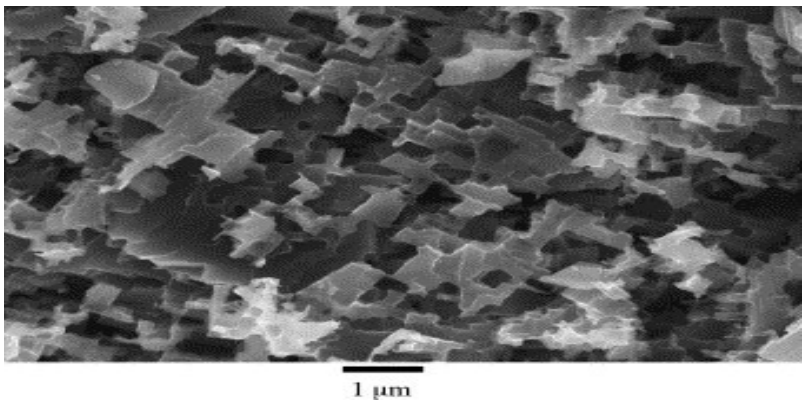

Fig. 1. FEG-SEM picture of an etched Al foil.

Secondly, the surface roughness of the Al is coated by a conducting film via the sol–gel route which is well known for its high covering power. The sol is constituted of a polymeric matrix with a conducting carbonaceous material; the sol viscosity is controlled. The polymeric matrix is prepared by condensation reactions between hexamethylenetetraamine (HMTA) and acetylacetone (Acac) in acetic acid. The sol–gel matrix allows to obtain a stable suspension of the carbonaceous particles in the sol. The particles have a lower size (50 nm) than the etching channels width created on the Al foil (a few µm). The slurry is deposited onto the Al substrate by dip-coating method with a controlled withdrawal speed in order to deposit the carbonaceous particles. A thermal treatment is performed in order to remove the polymeric matrix [19]. Fig. 2 represents a FEG-SEM picture of the Al foil covered by the carbonaceous slurry; the whole surface is covered by the carbonaceous particles. A homogeneous particle dispersion into the

channels is observed.

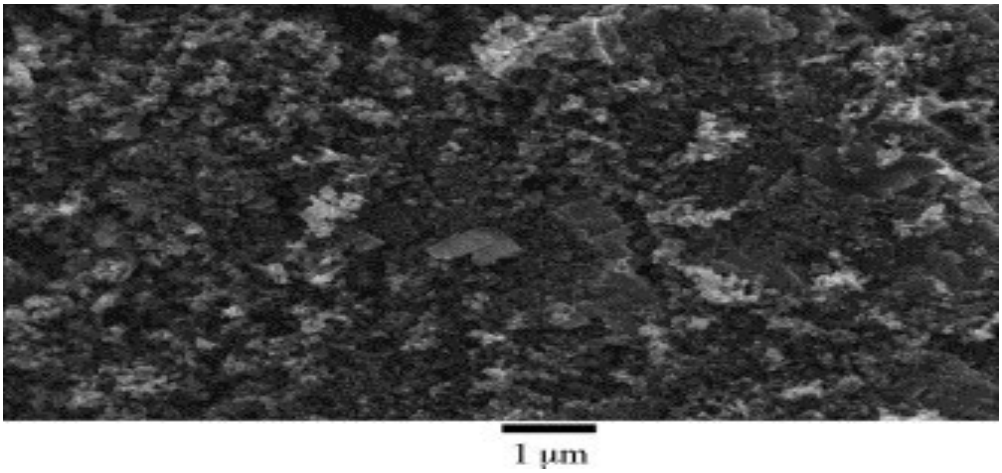

Fig. 2. FEG-SEM picture of an etched Al foil with a carbonaceous film.

2.3. Addition of CNTs in the active material

The influence of CNTs addition into the active material on the performances of Carbon/Carbon supercapacitors has been studied. DWNTs have been synthesised by a catalytic chemical vapour deposition (CCVD) from a mixture of CH_4 (18 mol%) in H_2 on a MgO-based catalyst, at a temperature of 1000 °C. The process has been described elsewhere [21] and [22]. Fig. 3 represents the FEG-SEM picture of CNTs sample; it can be seen that DWNTs form an important density of bundles and have extensive branching. Their diameter range is between 10 and 20 nm. No carbon nanofiber could be observed in the sample.

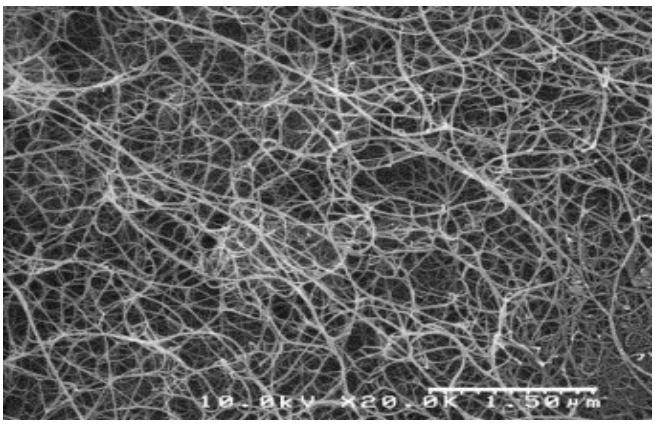

Fig. 3. FEG-SEM image of the raw sample of DWNTs.

Different compositions of the active material have been realised: x wt% activated carbon, y wt% CNT, 3 wt% CMC, 2 wt% PTFE where $x + y = 95$ and $y = 0$, 5, 10, 15 and 30%. Supercapacitors have then been assembled in the same way as described in Section 2.1.

2.4. Electrochemical apparatus

Galvanostatic cycling measurements have been performed with a BT2000 Arbin cycler at current

densities from 5 to 100 mA cm^{-2} between 0 and 2.3 V. Cell capacitance is calculated from the charge–discharge curves with an estimated error of ±1 F g^{-1} during cycling. The equivalent series resistance (ESR) is measured during a 1 ms pulse and the ESR value is obtained with an error value of 0.01 Ω cm^2. This ESR corresponds to the one measured at 1 kHz on the Electrochemical Impedance Spectroscopy plots, where the imaginary part $Z'' = 0$.

Electrochemical Impedance Spectroscopy (EIS) measurements were carried out with an EGG 6310 apparatus between 10 mHz and 50 kHz at a voltage of 2 V.

2.5. Specific capacitance calculation

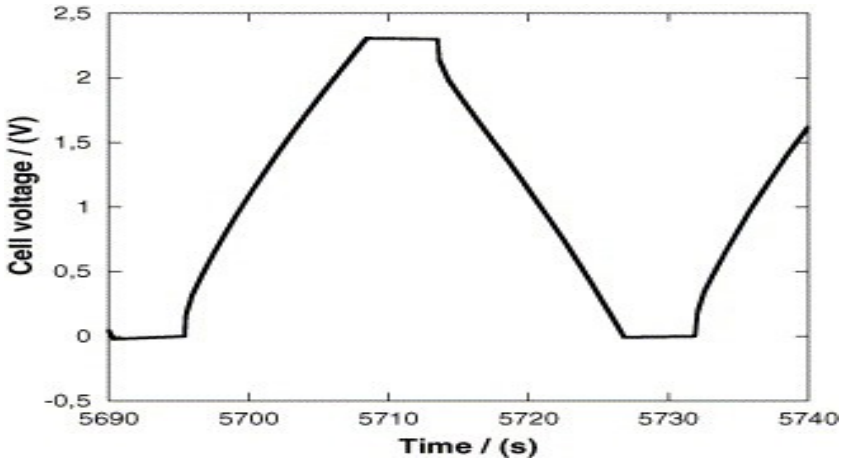

Fig. 4 presents the charge–discharge curve of a 4 cm^2 cell at constant current density ±100 mA cm^{-2}. The cell capacitance is deduced from the slope of the discharge curve:

(1)

where C is the cell capacitance in Farad (F), I the discharge current in Ampere (A) and dV/dt is the slope of the discharge curve in volts per second (V s^{-1}).

Fig. 4. Charge–discharge curve of a 4 cm^2 supercapacitor cell at j = ±100 mA cm^{-2}. Potentiostat holding at 0 and 2.3 V: 5 s.

The specific capacitance $C_{m\mathrm{AM}}$ in Farad per gram of active material (F g^{-1}) is related to the capacitance of the cell C by (2):

$$C = \frac{I}{\frac{dV}{dt}} \tag{2}$$

where m_{AM} is the weight (g) per electrode of the active material.

3. Results and discussion

3.1. 4 cm^2 supercapacitors assembled with treated Al current collector

Current collector/active material interface impedance contributes to increase the high frequency resistance and then the ESR; it has to be minimized. In this way, various surface treatments on current collectors have been proposed in the literature in order to improve the contact between the current collector and the active material of Carbon/Carbon supercapacitors in organic electrolyte. Maxwell [23] has patented a process which consists in a deposit of a pure Al layer by PVD on the active material. Lust et al. [24] proposed to spray a pure Al layer on the active material under vacuum. Du Pasquier et al. [25] used an adhesive conductive paint on the Al grid. Taberna et al. [26] vaporized a polyurethane conductive paint on Al collector foil by a spray method.

In a previous paper, 4 cm^2 cells assembled with etched Al foil with a carbonaceous sol–gel deposit were studied by Electrochemical Impedance Spectroscopy [19]. It was demonstrated that the sol–gel deposit leads to a decrease of the Al/active material interface resistance; this carbonaceous sol–gel deposit permits to increase the interface conductivity and to limit the contact of the electrolyte with the Al surface [19].

Here, performances of supercapacitors assembled with etched Al current collector with a carbonaceous film have been studied by galvanostatic cycling measurements between 0 and 2.3 V at ±100 mA cm^{-2}.

Performances obtained remain stable over 10,000 cycles: the ESR value is 0.5 Ω cm^2 (Fig. 5). The specific capacitance is 95 F g^{-1} of activated carbon measured at a current density of 20 mA cm^{-2}. This low ESR value traduces the great efficiency of the surface treatment proposed here; it shows the high influence of the interface resistance between the Al and the active material on the performances of Carbon/Carbon supercapacitors. This surface treatment based on an original process allowed to improve the Al/active material interface properties by lowering the internal resistance so that the delivered power is increased.

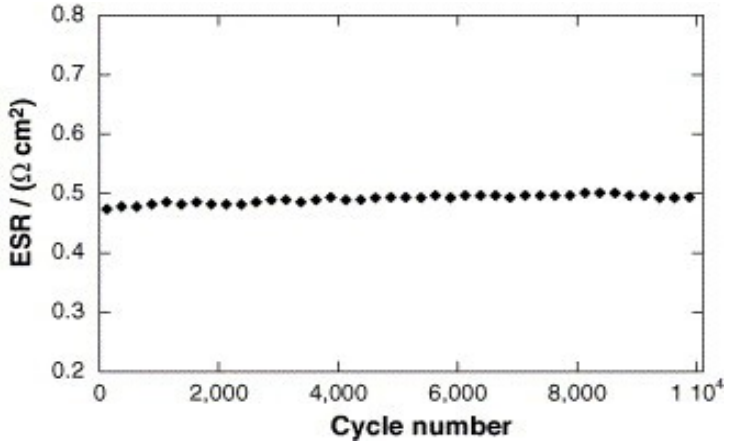

Fig. 5. Evolution of 4 cm^2 supercapacitor using etched Al foil with a carbonaceous coating and activated carbon-based electrodes.

3.2. 4 cm^2 supercapacitors assembled with treated Al current collector and active material containing activated carbon/CNTs mixture

CNTs are carbonaceous material with particular properties. They have higher electronic conductivity than activated carbon one [4] and [27], good electrochemical stability and a high accessible surface area. In the literature, performances of supercapacitors using CNTs based-electrodes in organic electrolyte exhibit low specific capacitances lower than the ones obtained in aqueous media [28] and [29].

In this paper, an active material of activated carbon/CNTs mixture with different composition is used in order to take advantages from these two carbonaceous materials. The influence of the addition of CNTs in the active material on the performances of 4 cm^2 supercapacitor cell using treated Al foil was studied by galvanostatic cycling measurements. Fig. 6 represents the ESR variation with the CNTs content in the active material measured during constant charge–discharge current density. For 5 and 10% CNTs content, the ESR is slightly decreased as compared to a supercapacitor containing pure activated carbon. For 15% CNTs content, the ESR is about 0.4 Ω cm^2 and very slightly decreases for 30% of CNTs. The modification of the ESR would be due to the presence of CNTs which improve both ionic and electronic conductivity. CNTs allow to lower electronic resistance of the active material and improve ionic conductivity of the electrolyte in the porous structure of the electrode. Fig. 7(a) represents the FEG-SEM picture of an active material containing 15% of CNTs; CNTs are homogeneously dispersed into the active material. It can be seen that DWNTs form bundles on the activated carbon grains. Fig. 7(b) shows that CNTs linked activated carbon grains; some of them connect the porous activated carbon to each other.

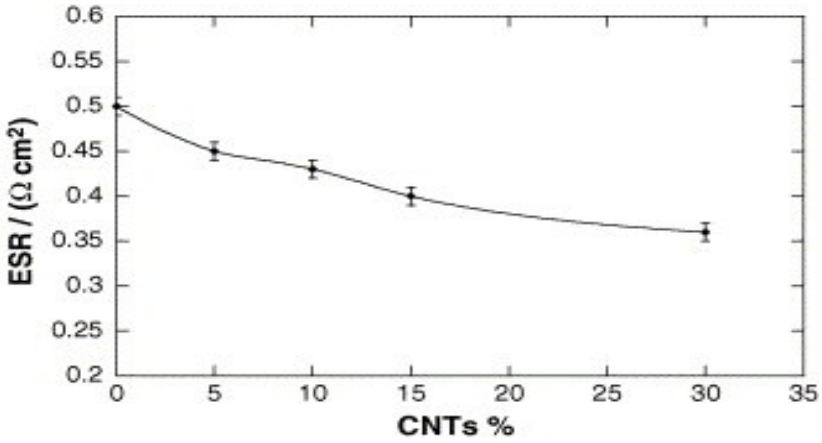

Fig. 6. Variation of internal resistance of 4 cm^2 supercapacitors cells assembled with treated Al foil and active material containing different CNTs content.

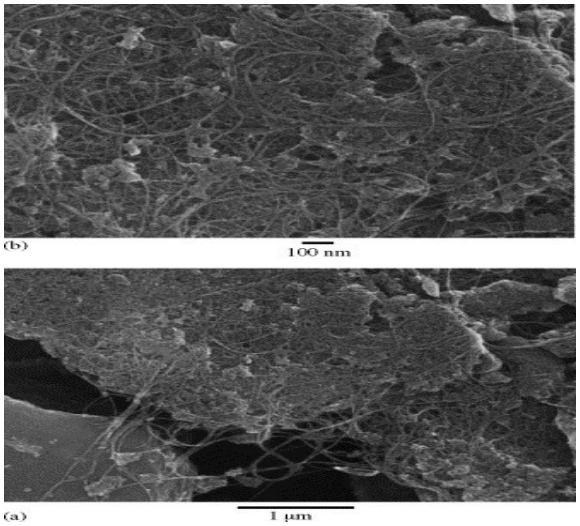

Fig. 7. FEG-SEM picture of active material containing 15% of CNTs. (a) CNTs bundles on the activated carbon grains. (b) Linkage of activated carbon grains by CNTs.

Fig. 8 represents the specific capacitance measured at a constant current density of 20 mA cm^{-2}. From 5 to 15% CNTs content in the active material, the specific capacitance is not so decreased as compared to a supercapacitor assembled with electrodes containing pure activated carbon. Beyond 15% of CNTs, a significant decrease of the capacitance is observed (up to 87 F g^{-1}). Emmenegger et al. showed that the cell capacitance of CNTs-based electrode increases with the electrode thickness [30]. For high CNTs content in the active material, electrode thickness increases but specific capacitance is lowered. This can be explained by a decrease of the surface area developed by CNTs bundles (985 m^2 g^{-1}) as compared to the surface area developed by the activated carbon (2300 m^2 g^{-1}).

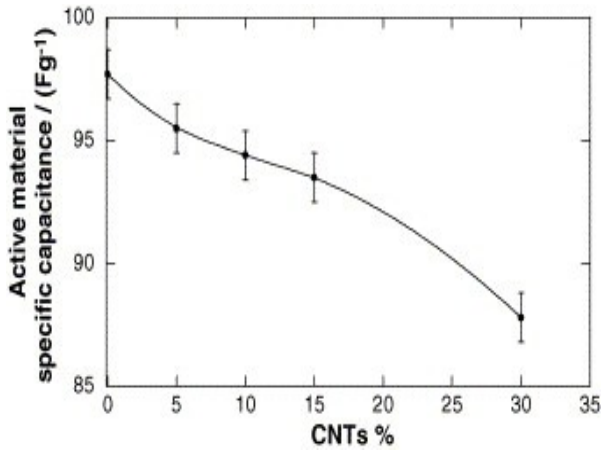

Fig. 8. Change of the specific capacitance measured at 20 mA cm^{-2} with the CNTs content in the active material.

Fig. 9 plots the change of the relative capacitance C/C_0 with the current densities. For low current densities (5 mA cm^{-2}), the specific capacitance (C_0) is maximum because of the lower ohmic drop (linked to the electronic and ionic resistance): the whole porosity in the electrode depth can be fully used for ion adsorption. By increasing the current density, a potential distribution appears across the inter-electrode spacing due to a porous structure of the electrode. The ohmic drop limits the double layer charging in the electrode depth. Only the outer part of the electrode is active leading to a capacitance loss [31] (*RC* network [6]). For a pure activated carbon cell, the capacitance loss is about 10% between 5 and 100 mA cm^{-2}. When CNTs are added into the active material, the same behaviour can be observed but the capacitance becomes less dependent with the current density. For CNTs content higher than 15%, the loss of capacitance is only less than 3%. This can be explained by a large decrease of the ESR because of the potential distribution is lower: the porous electrode gets a homogeneous potential distribution in the whole porosity. For high CNTs content, the capacitance is stabilized at higher current densities.

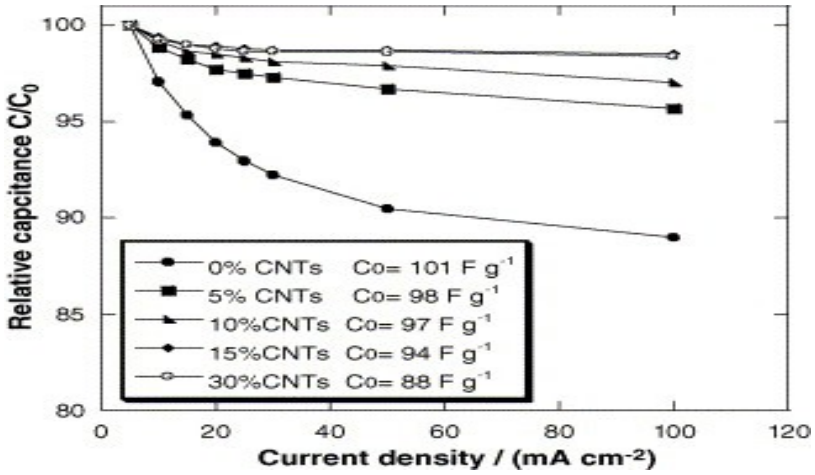

Fig. 9. Relative capacitance C/C_0 vs. the current for 4 cm^2 supercapacitors assembled with different CNTs content; C_0 represents the capacitance measured at 5 mA cm^{-2}.

The value of 15% CNTs appears as a good compromise between energy storage and delivering power; the decrease of the ESR from 0.5 down to 0.4 Ω cm^2 leads to an increase of delivered power (110 kW kg^{-1} of active material) without a large decrease of the specific capacitance. Fig. 10 shows the ESR change of a supercapacitor assembled with treated Al foil and 15% CNTs content over 10,000 cycles; the performances remains stable during galvanostatic cycling at a current density of 100 mA cm^{-2} with a stabilization of the ESR and a specific capacitance of 90 F g^{-1} of carbonaceous active material.

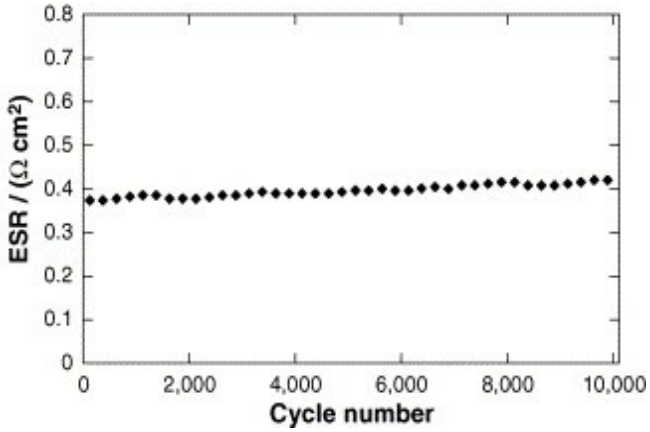

Fig. 10. Evolution of the ESR of 4 cm^2 supercapacitor assembled with treated Al foil and active material containing 15% of CNTs between 0 and 2.3 V at a constant current of 100 mA cm^{-2}.

3.3. Electrochemical Impedance Spectroscopy measurements

The frequency behaviour has been studied by EIS at a bias voltage of 2 V between 10 mHz and 50 kHz. Fig. 11 presents the Nyquist plot of 4 cm^2 supercapacitor cell assembled with active material containing pure activated carbon [19], 15 and 30% of CNTs. For high frequencies, the supercapacitor is mainly resistive. With lowering the frequency, Nyquist plot exhibits a "Warburg like" behaviour (insert, Fig. 11(b)) which traduces the ion penetration in the thickness of the porous structure of the electrode (*RC* network distribution) [6]. At low frequencies, the vertical

shape traduces a pure capacitor-like behaviour [32].

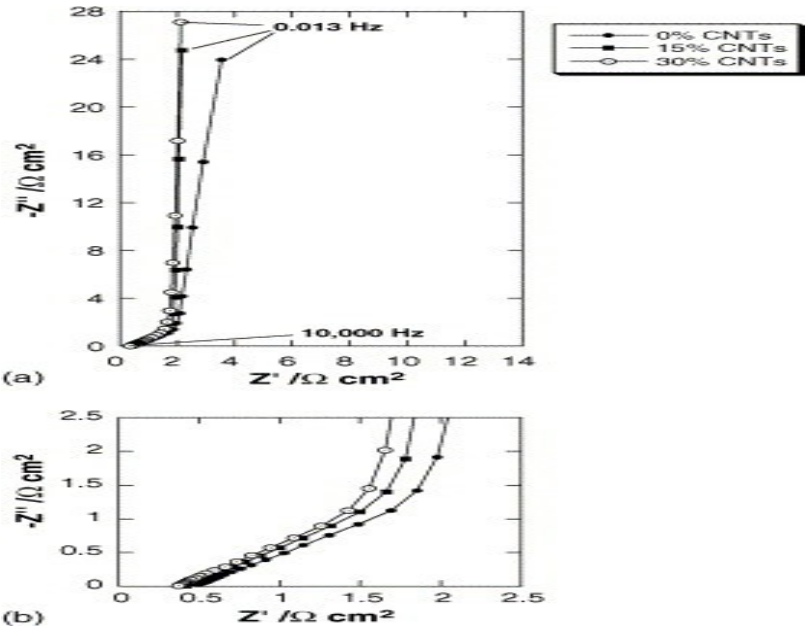

Fig. 11. (a) Nyquist plot of 4 cm^2 supercapacitor assembled with etched Al with a carbonaceous coating and active material no containing CNTs, 15 and 30% CNTs between 10 mHz and 50 kHz at a bias voltage of 2 V; (b) zoom of the Warburg frequency range.

The impedance frequency behaviour was studied using the complex model of the capacitance [26]. The cell capacitance is separated in two parts according to:

$$C=C'-jC'' \tag{3}$$

with:

$$C'(\omega) = \frac{-Z''(\omega)}{\omega|Z(\omega)|^2} \tag{4}$$

$$C''(\omega) = \frac{Z'(\omega)}{\omega|Z(\omega)|^2} \tag{5}$$

where C' represents the real part of the cell capacitance and C'' the imaginary part related to the losses in the charge storage process leading to an energy dissipation.

Fig. 12(a) represents the variation of the real part of the capacitance C' with the frequency. When CNTs are added in the active material, the low-frequency capacitance C_{LF} decreases; C_{LF} is the cell capacitance and corresponds to the one measured at low current density cycling. C_{LF} is maximum for a cell using pure activated carbon and decreases for higher CNTs content which is consistent with previous galvanostatic cycling results. It can be seen in Fig. 12(a) that C_{LF} is not largely affected in the frequency range studied (10 mHz–50 kHz) and the frequency behaviour is nearly the same for all the cells. C_{LF} is less frequency dependent at low frequency for high CNTs content; this observation appears more clearly in Fig. 12(b and c).

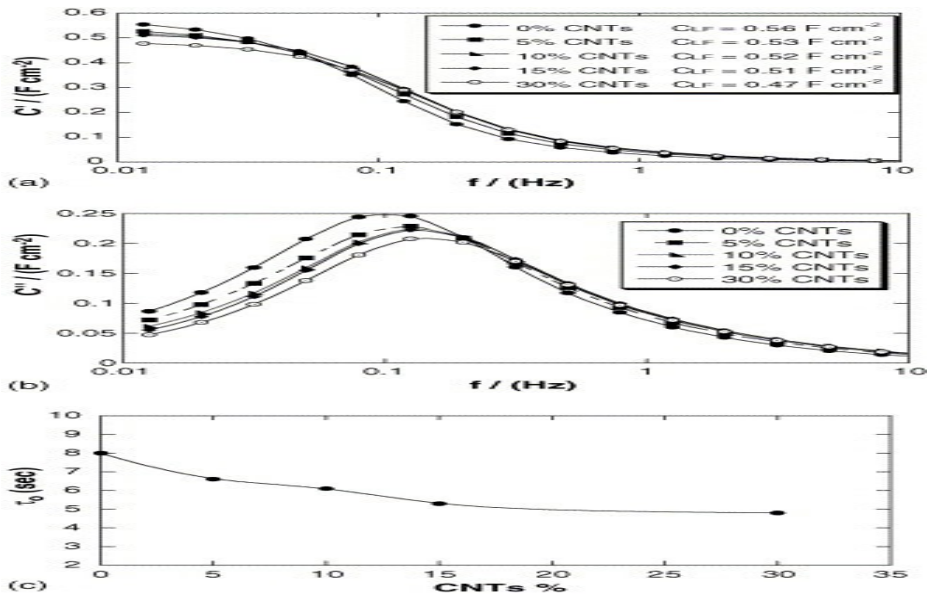

Fig. 12. (a) Evolution of the real part of the capacitance vs. the frequency with the CNTs content in the active material. (b) Evolution of the imaginary part of the capacitance vs. the frequency with the CNTs content in the active material. (c) Evolution of the relaxation time constant with the CNTs content in the active material.

Fig. 12(b) represents the variation of the imaginary part of the capacitance with the frequency. Fig. 12(c) plots the change of the relaxation time constant τ_0 with the CNTs content. τ_0 is characteristic of the system and is obtained for a frequency f_0 with $\tau_0 = 1/f_0$. From Fig. 12(a), f_0 corresponds to $C' = C_{LF}/2$; τ_0 separates the capacitive behavior ($C' > C_{LF}/2$) and the resistive behavior ($C' < C_{LF}/2$) of the supercapacitor. From Fig. 12(b), f_0 corresponds to the maximum energy dissipation. The time constant decreases when the CNTs content increases in the active material. For a supercapacitor using activated carbon-based electrodes, the relaxation time is 8 s; from the value of 15% CNTs, τ_0 tends to be stabilized around 4.9 s. For high CNTs content, i.e. 15 and 30%, the relaxation time constant is lowered about one-third as compared to a cell without CNTs. This lower time constant means that supercapacitors using high CNTs content are able to deliver higher power. The capacitive behaviour is shifted to higher frequencies for high CNTs contents.

Fifteen percent of CNTs in the active material seems then to be the optimum value in terms of power (low τ_0) and energy (high capacitance). This type of supercapacitor will be able to deliver the stored energy at higher power. Supercapacitors using electrodes with high CNTs content in the active material are suitable to be used as high power devices.

4. Conclusion

This paper presents performances obtained with 4 cm^2 Carbon/Carbon supercapacitors cells using treated Al current collector and active material containing activated carbon/carbon Nanotubes mixture in organic electrolyte (1.5 M NEt_4BF_4 in acetonitrile).

A surface treatment on Al foil has been proposed; it consists of an etching process followed by a carbonaceous sol–gel deposit. This process improved the surface contact between Al and active material leading to a decrease of the ESR. Performances obtained by galvanostatic cycling measurements present a low ESR value of 0.5 Ω cm^2 with a high specific capacitance (95 F g^{-1});

these performances remain stable over 10,000 cycles.

Performances of supercapacitors assembled with treated Al foil and active material containing activated carbon/CNTs mixture with different composition were then studied by galvanostatic cycling measurements. For low CNTs content, i.e. 5 and 10%, the internal resistance and specific capacitance slightly decrease as compared to a cell using activated carbon based electrodes. For 15% CNTs, the ESR is improved as compared to the cell reference leading to an increase of the delivering power (0.4 Ω cm^2) and the specific capacitance is 93 F g^{-1}. For 30% CNTs, the ESR very slightly decreases but the specific capacitance strongly decreases. Fifteen percent appears to be the best value in terms of energy and power performances.

In the third part, the frequency behaviour of the cells was studied by Electrochemical Impedance Spectroscopy measurements using the complex model of the capacitance. The relaxation time constant τ_0, also called factor of merit, is lowered when CNTs content in the active material is increased leading to a higher delivered power. Best results were obtained with 15% of CNTs content in the active material.

Supercapacitors assembled with etched Al foil with a carbonaceous sol–gel deposit and active material containing activated carbon and 15% of CNTs exhibit good performances, with an ESR of 0.4 Ω cm^2 and a specific capacitance of 93 F g^{-1} of active material.

Acknowledgment

The authors want to thank the “Délégation Générale pour l’Armement” for financial support of this work.

References

A. Burke, *J. Power Sources* **91** (2000), p. 37.

Y. Takamuku, Y. Ito and J. Ozaki, *International Conference on Advanced Capacitors* Kyoto, Japan, May 29–31 (2003).

Q.L. Fang, D.A. Evans, S.L. Roberson and J.P. Zheng, *J. Electrochem. Soc.* **148** (2001), p. A833.

J. Jiang and A. Kucernak, *Electrochim. Acta* **47** (2002), p. 2381.

M. Mastragostino, C. Arbizzani and F. Soavi, *Solid State Ionics* **148** (2002), p. 493.

W.-C. Chen, T.-C. Wen and H. Teng, *Electrochim. Acta* **48** (2003), p. 641.

D. Lozano-Castello, D. Carzorla-Amoros, A. Linares-Solano, S. Shiraishi, H. Kurihara and A. Oya, *Carbon* **41** (2003), p. 1765.

J. Gamby, P.L. Taberna, P. Simon, J.F. Fauvarque and M. Chesneau, *J. Power Sources* **101** (2001), p. 109.

A. Laforgue, P. Simon, J.F. Fauvarque, M. Mastragostino, F. Soavi, J.F. Sarrau, P. Lailler, M. Conte, E. Rossi and S. Saguatti, *J. Electrochem. Soc.* **150** (2003), p. A645.

A. Du Pasquier, I. Plitz, S. Menocal and G. Amatucci, *J. Power Sources* **115** (2003), p. 171.

A. Chu and P. Braatz, *J. Power Sources* **112** (2002).

R. Kötz and M. Carlen, *Electrochim. Acta* **45** (2000), p. 2483.

E. Frackowiak, K. Jurewicz, K. Szostak, S. Delpeux and F. Béguin, *Fuel Process. Technol.* **77-78** (2002), p. 213.

Ch. Emmeneger, P. Mauron, A. Züttel, Ch. Nützenadel, A. Schneuwly, R. Gallay and L. Schlapbach, *Appl. Surf. Sci.* **162163** (2000), p. 452.

A.K. Chatterjee, M. Sharon, R. Nanerjee and M. Neumann-Spallart, *Electrochim. Acta* **48** (2003), p. 3439.

E. Frackowiack and F. Béguin, *Carbon* **40** (2002), p. 1775.

K.H. An, K.K. Jeon, J.K. Heo, S.C. Lim and D.J. Bae, *J. Electrochem. Soc.* **149** (2002), p. A1058.

Q. Jiang, M.Z. Qu, G.M. Zhou, B.L. Zhang and Z.L. Yu, *Mater. Lett.* **57** (2002), p. 988.

C. Portet, P.L. Taberna, P. Simon and C. Laberty-Robert, *Electrochim. Acta* **49** (2004) (6), p. 905.

R.S. Alwitt, H. Uchi, T.R. Beck and R.C. Alkire, *J. Electrochem. Soc.* **131** (1984), p. 13.

E. Flahaut, R. Bacsa, A. Peigney and Ch. Laurent, *Chem. Commun.* (2003), p. 1442.

E. Flahaut, A. Peigney, Ch. Laurent and A. Rousset, *J. Mater. Chem.* **10** (2000), p. 249.

Maxwell Technology Patent, A. Nishino, U.S. Patent 4,621,607 (1985).

E. Lust, A. Jänes and M. Arullep, *J. Electroanal. Chem.* **562** (2004), p. 33.

A. Du Pasquier, J.A. Shelburne, I. Plitz, F. Badway, A.S. Gozdz and G.G. Amatucci, *Proceedings of the 11th International Seminar on Double-Layer Capacitors and Similar Energy Storage Devices* Deerfield Beach, FL, December 3–5 (2001).

P.L. Taberna, P. Simon and J.F. Fauvarque, *J. Electrochim. Soc.* **150** (2003), p. 292.

J. Wei, H. Zhu, B. Jiang, L. Ci and D. Wu, *Carbon* **41** (2003), p. 2495.

S. Shiraishi, H. Kurihara, K. Okabe, D. Hulicova and A. Oya, *Electrochem. Commun.* **4** (2002), p. 593.

Q. Xio and X. Zhou, *Electrochim. Acta* **48** (2003), p. 575.

Ch. Emmenegger, Ph. Mauron, P. Sudan, P. Wenger, V. Hermann, R. Gallay and A. Züttel, *J. Power Sources* **124** (2003), p. 321.

W.G. Pell, B.E. Conway and N. Marincic, *J. Electroanal. Chem.* **491** (2000), p. 9

R. De Levie, *Electrochim. Acta* **8** (1963), p. 751.

Corresponding author. Tel.: +33 5 61 55 68 02; fax: +33 5 61 55 61 63.

Original text : Elsevier.com